In Fig. 1 I show the results of two sets of calculations. The first, to provide a baseline, is a calculation with a $Y_2^2$ pattern of heat flux to model the present day mantle. This pattern very closely matches the distribution of $|I|$ for the GAD model (Fig. 1). The second set consists of four calculations each with a $Y_2^0$ pattern of heat flux but with differing amplitude. These show that the distribution of $|I|$ becomes closer to that observed palaeomagnetically earlier than 250 Myr ago as the amplitude of the variations in heat flux is increased. The calculations all have a non-zero axial octupole term in addition to the axial dipole, with all other terms averaging to zero within one standard deviation. I note that the emergence of an axial octupole term rather than an axial quadrupole could be anticipated given the symmetry properties of the dynamo[21] (the historical field shows a strong bias towards odd harmonics) and the symmetry of the imposed heat flux variation.

These results demonstrate that by altering the pattern of lateral heat flux variations at the core–mantle boundary it is possible to find dynamos that generate magnetic fields with persistent axial octupoles. In other words, they indicate that the tenability of the GAD model is a function of the pattern of lateral heat flux variations at the core–mantle boundary. Without doubt, that pattern will have been different in the past, so I must conclude that it is unsafe to apply the GAD hypothesis earlier than 250 Myr ago. Indeed, it is no coincidence that the expected timescale for changes in the pattern of mantle convection is similar to the timescale on which we can test the GAD model, as the disappearance of sea floor is itself a manifestation of cycling or turnover of the mantle.

Several cautions must be raised regarding this study. First, because of the uncertain relationship between lowermost mantle heterogeneity and core–mantle boundary heat flux, I am unable to scale the amplitude of the heat flux variations to the Earth, though the amplitudes that I have considered here are not unreasonably large. Second, it is unreasonable to expect that the pattern of heat flux variations would have remained fixed throughout the Precambrian and Palaeozoic. However, suppose that occasionally as the pattern of mantle convection evolves, the lowermost mantle acquires a $Y_2^0$ signature which gives rise to an axial octupole in the magnetic field, and that at other times (such as the past 250 Myr) the field is close to a geocentric axial dipole. Then, averaging the field over a sufficiently long time interval (one that encompasses periods of $Y_2^0$ heat flux variation), we would see a bias towards low palaeomagnetic inclination. So, somewhat unexpectedly, the reason that the GAD hypothesis works well for the Cenozoic and Mesozoic may be simply that 250 Myr is too short a period over which to average the field to test the hypothesis adequately. □

Received 9 July 1999; accepted 17 March 2000.


1. Gilbert, W. *De Magnete* (London, 1600). Translation: Chiswick Press, London, 1900–1901).
2. McElhinny, M. & McFadden, P. *Paleomagnetism* (Academic, San Diego, 2000).
3. Kent, D. & Smethurst, M. Shallow bias of paleomagnetic inclinations in the Paleozoic and Precambrian. *Earth Planet. Sci. Lett.* **160,** 391–402 (1998).
4. Irving, E. Paleomagnetic and paleoclimatological aspects of polar wandering. *Geofisica Pura e Applicata* **33,** 23–41 (1956).
5. Evans, M. Test of the dipolar nature of the geomagnetic field throughout Phanerozoic time. *Nature* **262,** 676–677 (1976).
6. McElhinny, M. & Lock, J. IAGA paleomagnetic databases with Access. *Surv. Geophys.* **17,** 557–591 (1996).
7. Kuang, W. & Bloxham, J. An Earth-like numerical dynamo model. *Nature* **389,** 371–374 (1997).
8. Buffett, B., Huppert, H., Lister, J. & Woods, A. On the thermal evolution of the Earth's core. *J. Geophys. Res.* **101,** 7989–8006 (1996).
9. Cox, A. & Doell, R. Long period variations of the geomagnetic field. *Bull. Seismol. Soc. Am.* **54,** 2243–2270 (1964).
10. Hide, R. Motions of the Earth's core and mantle, and variations of the main geomagnetic field. *Science* **157,** 3784–3785 (1967).
11. Cox, A. The frequency of geomagnetic reversals and the symmetry of the nondipole field. *Rev. Geophys.* **13,** 35–51 (1975).
12. Bloxham, J. & Gubbins, D. The secular variation of the Earth's magnetic field. *Nature* **317,** 777–781 (1985).
13. Gubbins, D. & Bloxham, J. Morphology of the geomagnetic field and implications for the geodynamo. *Nature* **325,** 509–511 (1987).
14. Bloxham, J. & Gubbins, D. Thermal core–mantle interactions. *Nature* **325,** 511–513 (1987).
15. Zhang, K. & Gubbins, D. On convection in the Earth's core driven by lateral temperature variations in the lower mantle. *Geophys. J. Int.* **108,** 247–255 (1992).
16. Zhang, K. & Gubbins, D. Convection in a rotating spherical fluid shell with an inhomogeneous temperature boundary condition at infinite prandtl number. *J. Fluid Mech.* **250,** 209–232 (1993).
17. Sarson, G. R., Jones, C. A. & Longbottom, A. W. The influence of boundary region heterogeneities on the geodynamo. *Phys. Earth Planet. Inter.* **101,** 13–32 (1997).
18. Bloxham, J. The effect of thermal core-mantle interactions on the paleomagnetic secular variation. *Phil. Trans. R. Soc. Lond. A* **358,** 1171–1179 (2000).
19. Glatzmaier, G., Coe, R., Hongre, L. & Roberts, P. The role of the Earth's mantle in controlling the frequency of geomagnetic reversals. *Nature* **401,** 885–890 (1999).
20. Giardini, D., Li, X.-D. & Woodhouse, J. Three-dimensional structure of the Earth from splitting in free-oscillation spectra. *Nature* **325,** 405–411 (1987).
21. Gubbins, D. & Zhang, K. Symmetry properties of the dynamo equations for palaeomagnetism and geomagnetism. *Phys. Earth Planet. Inter.* **75,** 225–241 (1993).



### Acknowledgements

I thank P. Hoffman, K. Katari, D. Kent, A. Maloof, R. O'Connell, D. Schrag and L. Tauxe for useful conversations during this work. This work was supported by the NSF.


Correspondence and requests for materials should be addressed to the author (e-mail: jeremy_bloxham@harvard.edu).

# Early human occupation of the Red Sea coast of Eritrea during the last interglacial


**Robert C. Walter*, Richard T. Buffler†, J. Henrich Bruggemann‡§‖, Mireille M. M. Guillaume¶, Seife M. Berhe#, Berhane Negassi†☆, Yoseph Libsekal**††, Hai Cheng‡‡, R. Lawrence Edwards‡‡, Rudo von Cosel‖, Didier Néraudeau§§ & Mario Gagnon‖‖**

** Departmento de Geologica, Centro de Investigaciôn Científica de Educación Superior de Ensenada, km. 107 Carr. Tijuana-Ensenada, Ensenada, B.C., Mexico*
*† Institute for Geophysics, University of Texas, Austin, Texas 78712, USA*
*‡ Department of Marine Biology, University of Groningen, PO Box 14, 9750 AA Haren, The Netherlands*
*§ Department of Marine Biology and Fisheries, University of Asmara, Asmara, PO Box 1220, Eritrea*
*‖ Experimental Zoology Group, Wageningen Institute of Animal Sciences, Wageningen University, PO Box 338, 6700 AH Wageningen, The Netherlands*
*¶ Muséum National d'Histoire Naturelle, Laboratoire de Biologie des Invertébrés Marins et Malacologie, ESA 8044-CNRS, 55 rue de Buffon, 75005 Paris, France*
*# African Minerals Inc., PO Box 4588, Asmara, Eritrea*
*☆ Department of Mines, Ministry of Energy and Mines, PO Box 272, Asmara, Eritrea*
*** National Museum of Eritrea, PO Box 5284, Asmara, Eritrea*
*†† Archaeology Unit, University of Asmara, PO Box 1220, Asmara, Eritrea*
*‡‡ Department of Geology and Geophysics, University of Minnesota, Minneapolis, Minnesota 55455, USA*
*§§ Laboratoire de Paléontologie, Géosciences Rennes, Université de Rennes I, Campus de Beaulieu, avenue du Général Leclerc, 35042 Rennes cedex, France*
*‖‖ Department of Anthropology, University of Toronto, Toronto, Ontario M5S 3G3, Canada*


**The geographical origin of modern humans is the subject of ongoing scientific debate. The 'multiregional evolution' hypothesis argues that modern humans evolved semi-independently in Europe, Asia and Africa between 100,000 and 40,000 years ago[1], whereas the 'out of Africa' hypothesis contends that modern humans evolved in Africa between 200 and 100 kyr ago, migrating to Eurasia at some later time[2]. Direct palaeontological, archaeological and biological evidence is necessary to resolve this debate. Here we report the discovery of early Middle Stone Age artefacts in an emerged reef terrace on the Red Sea coast of Eritrea, which we date to the last interglacial (about 125 kyr ago) using U–Th**

**mass spectrometry techniques on fossil corals. The geological setting of these artefacts shows that early humans occupied coastal areas and exploited near-shore marine food resources in East Africa by this time. Together with similar, tentatively dated discoveries from South Africa[3] this is the earliest well-dated evidence for human adaptation to a coastal marine environment, heralding an expansion in the range and complexity of human behaviour from one end of Africa to the other. This new, widespread adaptive strategy may, in part, signal the onset of modern human behaviour, which supports an African origin for modern humans by 125 kyr ago.**

Our discovery of early Middle Stone Age (MSA) tools within an emerged reef terrace on the Red Sea coast of Eritrea (Fig. 1) expands on earlier reports of artefacts found on the surface of Pleistocene marine deposits elsewhere on the African coast of the Red Sea[4–6]. Africa is the main source of fossils and artefacts bearing on the study of early hominid evolution, but the Middle to Upper Pleistocene—a period which has great potential for resolving the debate about the origins of modern humans—is largely unstudied as a result of the paucity of terrestrial exposures of the right age[7]. Now geological studies of near-shore marine deposits on the Red Sea coast of East Africa are helping to fill this gap[8] by showing that such coastal environments can yield important information about early human origins. Our discovery of bifacial handaxes—large, flat, teardrop-shaped tools flaked over at least part of both surfaces—together with obsidian flake and blade tools is unusual, indicating that old and new tool technologies were used at the time this reef formed.

The area we studied lies along the west coast of the Buri Peninsula (Fig. 1), which exposes a Pleistocene reef terrace near the village of Abdur. This terrace encompasses a 6.5 km by 1 km stretch of raised shoreline on the eastern coast of the Gulf of Zula (Fig. 2a). It is the fossil remnant of a N–S trending fringing reef, which consists of near-shore environments to the east, a central belt of fossil coral reefs, and offshore environments to the west. We subdivided Abdur into three geographic districts: Abdur South (AS), Abdur Central (AC) and Abdur North (AN) (Fig. 2a).

This Pleistocene reef terrace, termed here the Abdur Reef Limestone (ARL), originally formed in shallow water as a shell and coral biostrome, a laterally extensive sheet-like mass of rock built by sedentary marine organisms and composed mainly of their remains. The top of the terrace now ranges in average elevation from about +6 m (above sea level) at Abdur South to +10 m at Abdur Central to +14 m at Abdur North. This general rise in elevation is due, in part, to regional NNW–SSE trending normal faults that step up, en echelon, to the northeast (Fig. 2a). A second group of smaller normal faults is observed that trend NNE–SSW, which might be related to local doming of the Abdur Volcanic Complex that underlies the ARL to the east. This doming apparently also caused seaward tilting of the terrace; about 5° at Abdur South and Abdur Central, and about 1–2° at Abdur North.

The ARL is composed of 1–5 m thick build-ups of molluscs, corals, echinoderms and bioclastic sands. At Abdur North the reef is built mainly on older sedimentary rocks, named here the Buri Sequence, which consist of a succession of shallow marine, fluvial and lacustrine sediments more than 10 m thick that were faulted and deformed prior to deposition of the ARL (Fig. 2a and b). To the east, along its landward fringes, the reef laps onto the Abdur Volcanic Complex (Fig. 2a), which in turn overlies the Buri Sequence. To the south, at Abdur Central and Abdur South, the reef laps onto the volcanic complex, but the underlying Buri Sequence is not exposed.

Abdur North is the most laterally extensive and best studied of the

**Table 1 U–Th dated last interglacial terraces from the Red Sea coast of the Sinai Peninsula and Africa**

| Reference | Location | | Terrace height (m asl) | | U–Th age (kyr) | |
|---|---|---|---|---|---|---|
| | Name | Latitude | min | max | min | max |
| | Sinai | | | | | |
| 11 | Suweira | 28° 17′ | 5 | 18 | 119 | 134 |
| | Mureikha | 27° 56′ | 13 | 18 | 125 | 132 |
| | Point 28 | 27° 53′ | 5 | 8 | 120 | |
| | Umm-Sid | 27° 50′ | 13 | 18 | 81 | 127 |
| 12 | Gulf of Aqaba | 27° 43′ | 3 | 6 | 118 | 125 |
| | Egypt | | | | | |
| 6 | Ras Dib | 28° 05′ | 13 | 18 | 115 | 127 |
| | Gebel Zeit | 27° 55′ | 12 | 18 | 117 | 131 |
| | Zeituna | 27° 50′ | 11 | | 119 | 126 |
| | Ras Bahar | 27° 48′ | 5 | 8 | 123 | 126 |
| | Ras Gemsa | 27° 40′ | 10 | 14 | 125 | |
| | Q. el Qadim | 26° 10′ | 7 | 8 | 121 | |
| | S. el Bahari | 25° 55′ | 7 | | 121 | |
| | Wadi Nahari | 25° 00′ | 6 | | 118 | |
| | Wadi Igla | 25° 15′ | 10 | | 115 | |
| | W. K. el Bahari | 24° 40′ | 8 | | 120 | |
| | Red Sea Islands | | | | | |
| 13 | Brothers | 26° 18′ | 6 | 8 | 125 | |
| | Zabargad | 23° 37′ | 6 | 8 | 126 | |
| | Sudan | | | | | |
| 14 | Marub | ? | 3 | | 134 | |
| | Arkiai | 20° 10′ | 3 | | 128 | |
| | Awaitir | 20° 08′ | 4 | | 132 | |
| | Arus | 20° 00′ | 3 | | 142 | |
| | Irayes | 19° 55′ | 2 | 6 | 125 | 136 |
| | Eritrea | | | | | |
| 15 | Dahlak Kebir | 15° 45′ | 5 | | 117 | 170 |
| This study | Abdur | 15° 09′ | 6 | 14 | 118 | 136 |
| | Djibouti | | | | | |
| 16 | Fagal | 12° 26′ | 3 | | 110 | 125 |
| | Wayed Kibo | 11° 57′ | 3 | 12 | 124 | 133 |
| | Helento | 11° 52′ | 13 | | 123 | |
| 17 | Baie Beheta | ? | 1 | 9 | 105 | 120 |
| | Kala 'assa | 13° 10′ | 2 | 3 | 137 | |
| | Tadjura | 11° 50′ | 32 | | 116 | |
| | Obock | 11° 56′ | 20 | | 136 | |
| | Djibouti | 11° 30′ | 9 | | 126 | 142 |

m asl, metres above sea level. These dates indicates modest, but variable, tectonic uplift of the Red Sea coast over the last 125 kyr, accounting for current terrace elevations that are slightly above the estimated height of sea level during the last interglacial period: estimates for the height of the Red Sea during the last interglacial vary from +3 m to +8 m (refs 6, 14 and 18).

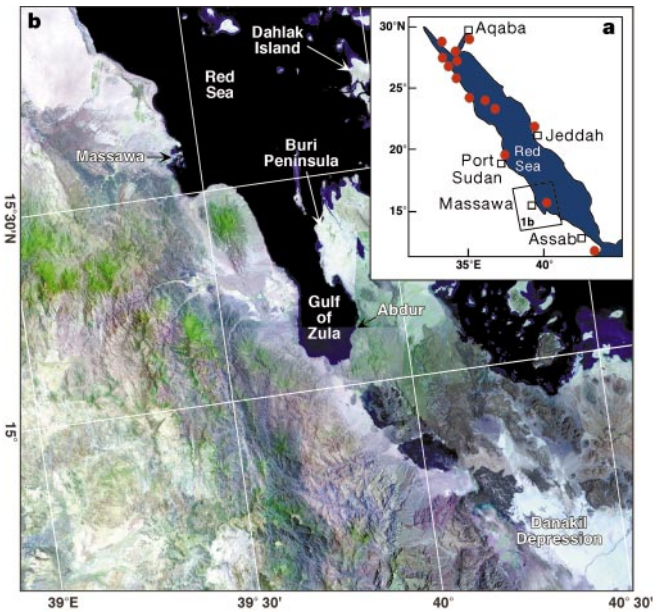


**Figure 1** The study area. **a**, Map of the Red Sea basin after ref. 18. Filled circles depict approximate locations of last interglacial coral terraces of the Red Sea (see Table 1). **b**, A 7-4-2 Landsat Thematic Mapper image of the study area. The Abdur Reef Limestone and the archaeological sites discussed here are located on the Gulf of Zula coast near the village of Abdur (arrow). (Scale: 30 minutes in latitude = 55 km). Figure courtesy of M. Abdelsalam, University of Texas at Dallas.

three geographic districts (Fig. 2a). Thirteen stratigraphic sections were measured, and faunal samples were collected from seven representative sections. Here the ARL is composed of the 0.5–3.1 m thick 'lower shell zone', which grades upward into the 0.5–1.5 m thick 'upper coral zone'. Present over much of the area at the base of the ARL, immediately below the lower shell zone, is a distinctive 15–30 cm thick cobble lag deposit consisting of locally derived limestone and volcanic clasts in a carbonate sand matrix. The 'basal cobble zone' overlies an irregular erosional surface, an angular unconformity, that truncates the underlying, tilted Buri Sequence. This lag formed during marine transgression when high-energy wave activity winnowed away finer particles, leaving the coarse cobbles behind. As water depth increased during the transgressive cycle the cobbles submerged into a restricted, quiet bay as an anchorable substrate suitable for growth of rich oyster beds.

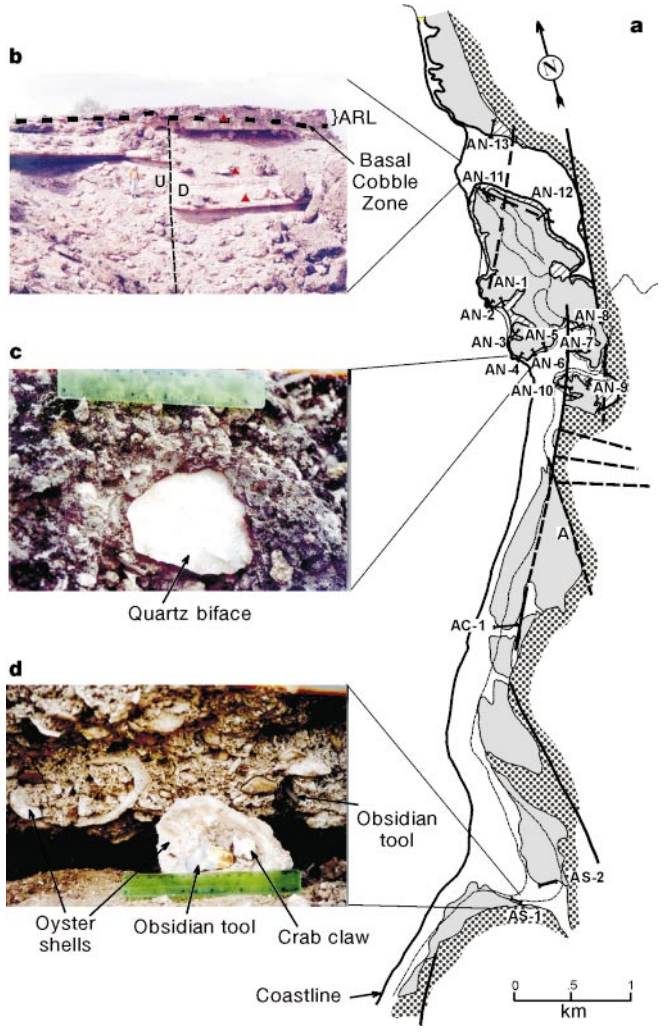


**Figure 2** Archaeological finds and their locations. **a**, Geological map of the Abdur field area, showing the location of measured stratigraphic sections (for example, AN-1). Abdur Reef Limestone (ARL), shaded; Abdur Volcanic Complex, dots; Buri Sequence, crosshatch; Faults, heavy lines (dashed where inferred); A, location of Abdur village. **b**, View of section AN-11, showing the stratigraphic position of *in situ* obsidian MSA tools within the basal cobble zone and in the underlying Buri Sequence (triangles). Horizontal dotted line indicates the basal cobble zone. Vertical dashed line indicates a small, normal fault shown along strike (U, up; D, down); the prominent resistant layers are displaced by roughly 3 m across the fault. **c**, A quartz biface, found *in situ* in the lower shell zone of the ARL at AN-4. Scale is 15 cm. **d**, Obsidian tools (one heavily patinated), with oyster and crab parts, all found *in situ* in a coarse bioclastic sand at the base of the lower shell zone at AS-1. Scale is 15 cm.

The lower shell zone is composed of bivalves, gastropods, echinoids, and occasional crustaceans and corals. This zone varies from being nearly all whole shells cemented together without matrix, to being entirely composed of sand- and granule-sized fragments of broken shells. This variation occurs from location to location and vertically within sections. The ecology of mollusc and echinoid species suggests a soft, sandy substrate in a shallow to medium subtidal environment. Bivalves (*Tridacna maxima* and *Spondylus* cf. *marisrubris*) and gastropods (*Chicoreus ramosus*, *Cypraea limacina* and *Cypraea pantherina*) from the upper part of the lower shell zone indicate proximity to coral reefs.

The upper coral zone is composed of scleractinian corals together with subordinate bivalves, gastropods and echinoids. We interpret this zone to be a fringing reef that formed in a calm embayment, similar to reefs forming today in Massawa Bay (offshore of the port city of Massawa, Fig. 1b). The corals of this zone are: (1) scattered corals not in growth position (for example, Faviidae in AN-4), probably representing a sandy talus seaward of the fringing reef, in water depths of 3 to >8 m; or (2) fields of branching corals in growth position (for example, *Stylophora* sp., *Goniopora* sp., *Galaxea* spp. in AN-7), typical of a reef flat zone of a fringing reef system, in water depths of 0.5–3 m. This linear reef flat extends from AN-13 to AN-10 (Fig. 2a), in a N–S belt, parallel to the palaeoshoreline. It reappears to the south at AC-1 where it shows its best development.

Along the eastern edge of the ARL, near the ancient shoreline of the Buri Peninsula, the shell and coral zones give way laterally to a beach facies, which is 1–2 m thick, resistant carbonate-cemented coarse sand and gravel composed of broken shell fragments interspersed with locally derived gravels of volcanic rock. Scattered shells of oysters, giant clams and crustaceans are found in this facies, as are fossils of terrestrial mammals such as elephant, hippopotamus, rhinoceros and bovid (species not determined).

Abundant stone tools are found *in situ* in the basal cobble zone, the lower part of the lower shell zone and the beach facies of the ARL. At Abdur South, flakes and blades are found throughout the lower shell zone of section AS-1 (Fig. 2d), which here is a bioclastic sand with rich concentrations of separated valves of oysters and other bivalves, gastropods and crustaceans. At AS-2 and AC-1, *in situ* flakes and blades are found in the beach facies. At Abdur North *in situ* bifaces (similar in appearance to Acheulian hand axes[7,9,10]) are found at AN-1, AN-4 and AN-12, and flakes and blades are found *in situ* in the basal cobble zone, the lower part of the lower shell zone and/or in the beach facies at AN-1, AN-4, AN-7, AN-10, AN-11, AN-12 and AN-13. Bifaces are made primarily from fine-grained volcanic rocks, but also from chert and quartz (Fig. 2c). Flake and blade tools are made mainly from obsidian (Fig. 2d), but occasionally from chert and quartz. Potential sources of these raw materials are found within 1 to 20 km of Abdur.

Our initial estimate of the age of the tool-bearing ARL was 125 kyr, based on its relative height above present sea level. Coral terraces from the Red Sea coast of southern Sinai[11], Egypt[6,12], the Red Sea Islands[13], Sudan[14], the Dahlak Islands[15] and Djibouti[16,17] (Fig. 1a), all of which are about the same elevation as the ARL, date to around 125 kyr by U–Th alpha counting techniques (Table 1). The Red Sea is one of the best-dated Quaternary basins in the world. Fossil beaches and coral reefs of this age (about 115–135 kyr) were the most common landforms on the Red Sea coast[18] when sea level was 3–8 m higher than today (Table 1).

To confirm this estimate, approximately 100 coral samples were collected from the upper coral zone of the ARL for species identification and evaluation for dating. Twenty-four coral samples were subsequently selected for X-ray diffraction studies as possible candidates for U–Th mass spectrometry analyses. Six of the 24 samples yielded aragonite contents between 95% and 100%, all from Abdur North, suggesting that these corals could yield reliable U–Th ages. Four of the samples are from AN-4, one from AN-7 and

one from AN-13 (Fig. 2a), representing a wide distribution across the Abdur North terrace. These six samples were dated using thermal ionization mass spectrometry (TIMS) U–Th techniques (Table 2, refs 19 and 20).

Four coral samples from section AN-4 have primary uranium concentrations and initial uranium isotopic compositions similar to the modern marine value[20], suggesting that the dates are accurate. The dates range from 118 to 126 kyr ago, confirming that the ARL formed during the last interglacial high-stand[19,21,22], oxygen isotope substage 5e. A fresh quartz hand axe occurs *in situ* in the lower part of the lower shell zone of AN-4 (Fig. 2c), as well as several obsidian flake tools. Obsidian flake tools were also found at AN-4 in the basal cobble zone immediately below the lower shell zone.

The coral sample from section AN-7 yields a date of 136 kyr, slightly older than the dates from AN-4, but still within the temporal range for the last interglacial high-stand compared to other terraces on the Red Sea coast (Table 1). Obsidian flake tools were found in the lower part of the lower shell zone of section AN-7, stratigraphically below the dated coral.

The sample from section AN-13 yields a date of 156 kyr. This is probably erroneous because the uranium concentration is about half the lowest value for primary coralline aragonite (Table 2), which indicates either U loss from the coral or that the U–Th measurement was made on a portion of the coral that had a higher calcite (lower U) abundance than the portion analysed by X-ray diffraction. Either scenario invalidates the date. An erroneous age is suggested because the date of 156 kyr would place the coral in the period of the penultimate glaciation (oxygen isotope stage 6), when sea levels were about 130 m lower than today[23].

Five of six U–Th dates measured on *in situ* corals from Abdur North indicate that the ARL was deposited between 118 and 136 kyr (Table 2). This is consistent with U–Th ages measured on corals from the last interglacial highstand from the Red Sea basin (by alpha counting, Table 1) and from elsewhere (by TIMS[19,21,22]). A simple mean age for the Abdur Reef Limestone, calculated from the five best U–Th results, is 125 ± 7 kyr ($1\sigma$).

We conclude that the stone tools within the ARL are 125 ± 7 kyr old, as shown by their stratigraphic context within this last interglacial reef terrace. Even earlier coastal occupation at Abdur is suggested by the discovery of obsidian tools in the Buri Sequence below the ARL (Fig. 2b), but the age of these deposits is not yet known. The tools in the ARL have fresh, sharp edges, and they are found in low-energy environments. This indicates that the tools were not washed in from older sediments. Neither are they younger artefacts that 'filtered down' into the terrace after subaerial exposure, since the tools are found in the lower shell and cobble zones of the terrace and not in the upper coral zone. Such filtering is also precluded by the closely packed nature of the deposit itself.

The primary context is confirmed by the distribution of fresh stone tools within and throughout several reef facies over a wide area (Fig. 2a). Fresh bifaces and obsidian flakes and blades are found within the lower half metre of the lower shell layer (Figs 2c and d). The tools in the basal cobble zone have fresh, sharp edges, whereas the cobbles are subrounded. Hundreds of freshly preserved obsidian flake and blade tools are found in the beach rock, usually in close proximity to fossil remains of land mammals or near the massive oyster beds.

The simplest explanation for the occurrence of stone tools in the ARL is that whoever made the tools used them to harvest edible (energetically profitable and palatable) shallow marine molluscs and crustaceans and to butcher large land mammals near the shore of this reef system, and then discarded the tools at the various food processing sites. Two edible species of oysters are found in growth position as beds in the basal cobble and lower shell zones (*Hyotissa hyotis* and *Ostrea cf. deformis*). Thirty-one species of edible molluscs were identified from the lower shell zone. Two groups of decapod crustaceans were found in the basal cobble zone and the lower shell zone; one of these groups comprises big brachyuran crabs, which are edible.

Flake and blade tools from the ARL fit into the broad range of variability that defines the early Middle Stone Age (MSA)[7], but their stratigraphic association with Acheulian-type bifaces is unusual. Early MSA tools in Africa are generally found at sites where such bifaces are no longer present. However, there is currently no precise definition of what tools comprise the earliest MSA[7] tool-kit, or whether the biface—a tool that is generally associated with much older sites—is or is not part of this transitional assemblage.

The discovery of Palaeolithic artefacts in the Abdur Reef Limestone confirms and expands earlier reports of Acheulian-type tools found near emerged reef terraces from the central Danakil Depression[4] and the Egyptian coast of the Red Sea[5,6]. These earlier discoveries were not found in geological context, and consequently no firm assessment of their age is possible. The U–Th dates for the ARL artefacts, however, now permit us to link the Red Sea coast of Eritrea with several South African MSA sites that share evidence of stone tools associated with marine resource adaptations: Herold's Bay, Sea Harvest, Hoedjies Punt, Klasies River Mouth and Die Kelders' Cave[9,24,25]. The oldest of these, Klasies River Mouth and Herold's Bay, are tentatively dated to 115–100 kyr or correlated with oxygen isotope stage 5 based on geological grounds[3,24]. Archaic *Homo sapiens* were recently found at a coastal site in Greece, estimated to be about 200 kyr, but no stone tools are linked with the hominids and the date is speculative[26].

Archaeological evidence from the ARL confirms that the Red Sea coast of Africa was occupied by early humans by at least 125 kyr ago, but we cannot say, as yet, to which hominid species the tools belong. Human fossils from the last interglacial period at Klasies River Mouth are attributed to near or fully anatomically modern *Homo sapiens*[24]. Fossils from terrestrial sites of the East African interior, such as Lake Eyasi (~130 kyr), Mumba Rockshelter (~109–130 kyr), the Ngaloba Beds (~120 kyr) and Omo-Kibish (~130 kyr)[7], suggest that late archaic *Homo sapiens* and/or anatomically modern

**Table 2 $^{230}$Th ages and related data for aragonite coral samples form the Abdur Reef Limestone**

| Sample | Aragonite (%) | $^{238}$U (p.p.b.) | $^{232}$Th (p.p.t.) | $^{230}$Th/$^{238}$U (activity) | $^{230}$Th Age (kyr) | $\delta^{234}$U (initial) |
|---|---|---|---|---|---|---|
| AN-4-1a no. 1 | 99 | 3167 (4) | 1309 (11) | 0.7550 (19) | 118.9 (0.6) | 167.5 (1.8) |
| AN-4-1a no. 1 | 99 | 3287 (4) | 374 (10) | 0.7492 (20) | 117.2 (0.6) | 167.3 (1.8) |
| | | | | Average 118.1 (1.0) | | |
| AN-4-1a no. 2 | 100 | 3071 (4) | 101 (7) | 0.7678 (19) | 124.0 (0.6) | 160.7 (1.6) |
| AN-4-13a no. 1 | 96 | 3153 (4) | 991 (12) | 0.7537 (18) | 119.0 (0.6) | 164.8 (1.7) |
| AN-4-13a no. 3 | 98 | 3433 (5) | 46 (7) | 0.7768 (20) | 125.9 (0.7) | 166.1 (1.8) |
| AN-7-6a no. 2 | 98 | 2400 (3) | 437 (9) | 0.8111 (20) | 136.4 (0.7) | 172.1 (2.0) |
| AN-13-16a no. 6 | 95 | 1280 (1) | 4025 (15) | 0.8597 (20) | 156.0 (0.9) | 170.0 (1.9) |

Half lives are those quoted in ref. 20. Numbers in parentheses are $2\sigma$ errors. A simple mean age for the Abdur Reef Limestone, calculated from the five best U–Th results, is 125 ± 7 kyr; see text for details. Inclusion of the 156 kyr date, which we consider to be erroneous, would make the spread of ages larger than expected for oxygen isotope substage 5e compared to other terraces from the Red Sea (Table 1), except for the Dahlak Islands — the closest of the previously dated terraces to Abdur (Fig. 1 and Table 1).

humans were in East Africa by the time the ARL was forming. Thus, the stone tools from the ARL overlap in time with the apparent transition from archaic to modern *Homo sapiens* in Africa.

Regardless of which hominid species made the tools at Abdur, or at the more tenuously dated sites in South Africa, the pressing question is: what caused such an apparently sudden and widespread coastal marine adaptation by early humans by the last interglacial period? Climate changes leading to hyper-arid conditions in Africa and the Red Sea basin during the penultimate glaciation (~150 kyr) and at the peak of the last interglacial[6,27,28] may have been severe enough to pressure early humans to migrate from once stable interior habitats to exploit coastal marine habitats for survival. As opposed to shrinking freshwater environments during these times (for example, East African rivers and lakes), human adaptation to marine shoreline environments might have been further influenced by the lack of competition from other terrestrial mammals for coastal marine food resources. It is likely, however, that during extreme hyper-arid conditions marking the peak of the penultimate glaciation, that the Red Sea basin itself was virtually uninhabitable.

Our working model is that: (1) an adaptation to coastal marine environments in Africa by 125 kyr marks a significant, new behaviour for early humans; (2) early humans adopted this strategy in response to environmental stresses caused by fluctuating glacial–interglacial climate cycles that were especially pronounced during the late Middle and early Upper Pleistocene; (3) the proliferation of this strategy by the last interglacial suggests that its first appearance was even earlier; (4) the eventual dispersal of humans out of Africa was due to increased human competition for marine resources, possibly during hyper-arid conditions; and (5) human populations dispersed along the Red Sea coast out of Africa into the Levant by 100 kyr ago[29], and perhaps across a landbridge between Africa and Arabia[30] at the southern end of the Red Sea that was exposed during sea-level lowstands that mark the last two glacial maxima[23]. The artefacts from the Abdur Reef Limestone are in the right geographical location and of the right age to suggest that the route out of Africa was along the coast of Eritrea. It is now clear that the Red Sea basin, and perhaps the entire eastern shoreline of Africa, must be examined for additional evidence to test this model of early human occupation of coastal marine environments before 100 kyr ago, and its role in the dispersal of early humans out of Africa. □

Received 13 December 1999; accepted 17 February 2000.


1. Thorne, A. & Wolpoff, M. The multiregional evolution of humans. *Sci. Am.* April, 28–33 (1992).
2. Stringer, C. B. The emergence of modern humans. *Sci. Am.* December, 98–104 (1990).
3. Deacon, H. J. in *The Human Revolution: Behavioural and biological perspectives on the origins of modern humans* (eds Mellars, P. & Stringer, C.) 547–564 (Princeton Univ. Press, 1989).
4. Faure, H. & Roubet, C. Découverte d'un biface Acheuléen dans les calcaires marins du golfe Pléistocène de l'Afar (Mer Rouge, Éthiopie). *C. R. Acad. Sci. Paris* **267,** 18–21 (1968).
5. Montenat, C. Un aperçu des industries préhistoriques du golfe de Suez et du littoral Égyptien de la Mer Rouge. *Bull. Inst. Fran. d'Archéol. Orien.* **86,** 239–255 (1986).
6. Plaziat, J.-C. *et al.* in *Sedimentation and Tectonics in Rift Basins: Red Sea-Gulf of Aden* (eds Purser, B. H. & Bosence, D. W.J.) 537–573 (Chapman & Hall, London, 1998).
7. Clark, J. D. The Middle Stone Age of East Africa and the beginnings of regional identity. *J. World Prehist.* **2,** 237–305 (1988).
8. Walter, R. C., Buffler, R. T., Berhe, S., Vondra, C. & Yemane, T. in *Lithospheric Structure, Evolution And Sedimentation In Continental Rifts (Abstracts)* (eds Jacob, A. W. B., Delvaux, D. & Khan, M. A.) (Dublin Institute for Advanced Studies, Dublin, Ireland, 1997).
9. Phillipson, D. W. *African Archaeology* (Cambridge Univ. Press, 1993).
10. Van Peer, P. The Nile corridor and the out-of-Africa model. *Curr. Anthropol.* **39,** 115–140 (1998).
11. Gvirtzman, G., Kronfeld, J. & Buchbinder, B. Dated coral reefs of the southern Sinai (Red Sea) and their implication to late Quaternary sea levels. *Mar. Geol.* **108,** 29–37 (1992).
12. El-Asmar, H. M. Quaternary isotope stratigraphy and paleoclimate of coral reef terraces, Gulf of Aqaba, south Sinai, Egypt. *Quat. Sci. Rev.* **16,** 911–924 (1997).
13. Hoang, C. T. & Taviani, M. Stratigraphic and tectonic implications of uranium-series dated coral reefs from uplifted Red Sea islands. *Quat. Res.* **35,** 264–273 (1991).
14. Hoang, C. T., Dalongeville, R. & Sanlaville, P. Stratigraphy, tectonics and paleoclimatic implications of uranium-series dated coral reefs from the Sudanese coast of the Red Sea. *Quat. Int.* **31,** 47–51 (1996).
15. Conforto, L., Delitala, M. C. & Taddeucci, A. Datazioni col $^{230}$Th di alcune formazioni coralligene delle Isole Dahlak (Mar Rosso). *Soc. It. Min. Pet.* **32,** 153–158 (1976).
16. Hoang, C. T., Lalou, C. & Faure, H. Les récifs soulevés a l'ouest du golfe d'Aden (T. F. A. I.) et les hauts niveaux de coraux de la dépression de l'Afar (Éthiopie), géochronologie et paléoclimats interglaciaires. *Col. Int. CNRS* **219,** 103–116 (1974).
17. Faure, H., Hoang, C. T. & Lalou, C. Datations $^{230}$Th/$^{234}$U des calcaires coralliens et mouvements verticaux a Djibouti. *Bull. Soc. Géol. Fr.* **22,** 959–962 (1980).
18. Taviani, M. in *Sedimentation and Tectonics in Rift Basins: Red Sea-Gulf of Aden* (eds Purser, B. H. & Bosence, D. W. J.) 574–582 (Chapman & Hall, London, 1998).
19. Edwards, R. L., Chen, J. H. & Wasserburg, G. J. $^{238}$U-$^{234}$U-$^{232}$Th systematics and the precise measurement of time over the past 500,000 years. *Earth Planet. Sci. Lett.* **81,** 175–192 (1986/87).
20. Cheng, H. *et al. The half-lives of uranium-234 and thorium-230* (in the press).
21. Chen, J. H., Curran, H. A., White, B. & Wasserburg, G. J. Precise chronology of the last interglacial period: U-234-Th-230 data from fossil coral reefs in the Bahamas. *Geol. Soc. Am. Bull.* **103,** 82–97 (1991).
22. Stirling, C. H., Esat, T. M., Lambeck, K. & McCulloch, M. T. Timing and duration of the Last Interglacial: evidence for a restricted interval of widespread coral reef growth. *Earth Planet. Sci. Lett.* **160,** 745–762 (1998).
23. Gvirtzman, G., Buchbinder, B., Sneh, A., Nir, Y. & Friedman, G. Morphology of the Red Sea fringing reefs: a result of the erosional pattern of the last-glacial low-stand sea level and the following Holocene recolonization. *Mém. Bur. Rech. Géol. Min.* **89,** 480–491 (1977).
24. Klein, R. G. in *The Human Revolution: Behavioural And Biological Perspectives On The Origins Of Modern Humans* (eds Mellars, P. & Stringer, C.) 529–546 (Princeton Univ. Press, New Jersey, 1989).
25. Brink, J. & Deacon, H. A study of a last interglacial shell midden and bone accumulation at Herold's Bay, Cape Province, South Africa. *Paleoecol. Afr.* **15,** 31–39 (1982).
26. Leney, M. The road out of Africa. *Discov. Archaeol.* **1,** 18 (1999).
27. Freytet, R., Baltzer, F. & Conchon, O. A Quaternary piedmont on an active margin: the Egyptian coast of the NW Red Sea. *Z. Geomorph. N. F.* **37,** 215–236 (1993).
28. Horowitz, A. Continuous pollen diagrams for the last 3.5 m.y. from Israel: vegetation, climate and correlation with the oxygen isotope record. *Paleogeogr. Paleoclimatol. Paleoecol.* **72,** 63–78 (1989).
29. Grûn, R. & Stringer, C. B. Electron spin resonance dating and the evolution of modern humans. *Archaeometry* **33,** 153–199 (1991).
30. Leakey, L. *The Stone Age Cultures of Kenya Colony* (Cambridge Univ. Press, 1931).



### Acknowledgements

Permission to conduct field work was granted by the Department of Mines of the Ministry of Mines, Energy and Water Resources of Eritrea. We are grateful to A. Kibreab, T. Keleta, A. Mesfin and M. Abraha, G. Ogubazghi and B. Woldehaimanot, and the staff of the National Museum of Eritrea for their support. Financial support was provided by grants from Anadarko Petroleum Company, the National Science Foundation, the Institute of Human Origins, the Royal Ontario Museum and the University of Toronto. Donations by TOTAL Eritrea are gratefully acknowledged. We thank M. Kusmu, L. Le Vert, the French Ministry of Foreign Affairs, the Canadian Consulate and the US Embassy in Asmara. We also thank M. Abdelsalam, T. Andemariam, J. Aronson, B. Collins, C. Cermignani, M. Chazan, S. Churchill, D. Doumenc, E. Goodman, M. Gorton, D. Guinot, Y. Lam, A. Martyn, N. Mohammed, N.-H. Nguyen, J. Pandolfi, K. Reed, H. Shoshani, G. Smithwalter, R. Stern, M. Tesfaye, J. Trondle, M. de Saint Laurent, F. Taylor, G. Watson, C. Vondra and T. Yemane for assistance and/or discussions. Bifaces were first observed on the coast near Abdur by C. Hillman and reported to RCW. in 1995.


Correspondence and requests for materials should be addressed to R.C.W. (e-mail: rwalter@cicese.mx).

# The origin of red algae and the evolution of chloroplasts

**David Moreira*†, Hervé Le Guyader* & Hervé Philippe***

** Equipe Phylogénie et Evolution Moléculaires, CNRS UPRES-A 8080, Université Paris-Sud, Bâtiment 444,91405 Orsay Cedex, France*
*† Departamento de Microbiología, Universidad Miguel Hernández, Campus de San Juan, 03550 Alicante, Spain*

**Chloroplast structure and genome analyses support the hypothesis that three groups of organisms originated from the primary photosynthetic endosymbiosis between a cyanobacterium and a eukaryotic host: green plants (green algae + land plants), red algae and glaucophytes (for example, *Cyanophora*)[1]. Although phylogenies based on several mitochondrial genes support a specific green plants/red algae relationship[2,3], the phylogenetic analysis of nucleus-encoded genes yields inconclusive, sometimes contradictory results[3,4]. To address this problem, we have analysed an alternative nuclear marker, elongation factor 2, and included new red algae and protist sequences. Here we provide significant support for a sisterhood of green plants and red algae. This sisterhood is also significantly supported by a multi-gene analysis of a fusion of 13 nuclear markers (5,171 amino acids). In addition,**